Immunity, Volume *53*

Supplemental Information

SARS-CoV-2 Epitopes Are Recognized by a Public and Diverse Repertoire of Human T Cell Receptors

Alina S. Shomuradova, Murad S. Vagida, Savely A. Sheetikov, Ksenia V. Zornikova, Dmitry Kiryukhin, Aleksei Titov, Iuliia O. Peshkova, Alexandra Khmelevskaya, Dmitry V. Dianov, Maria Malasheva, Anton Shmelev, Yana Serdyuk, Dmitry V. Bagaev, Anastasia Pivnyuk, Dmitrii S. Shcherbinin, Alexandra V. Maleeva, Naina T. Shakirova, Artem Pilunov, Dmitry B. Malko, Ekaterina G. Khamaganova, Bella Biderman, Alexander Ivanov, Mikhail Shugay, and Grigory A. Efimov

Supplemental information

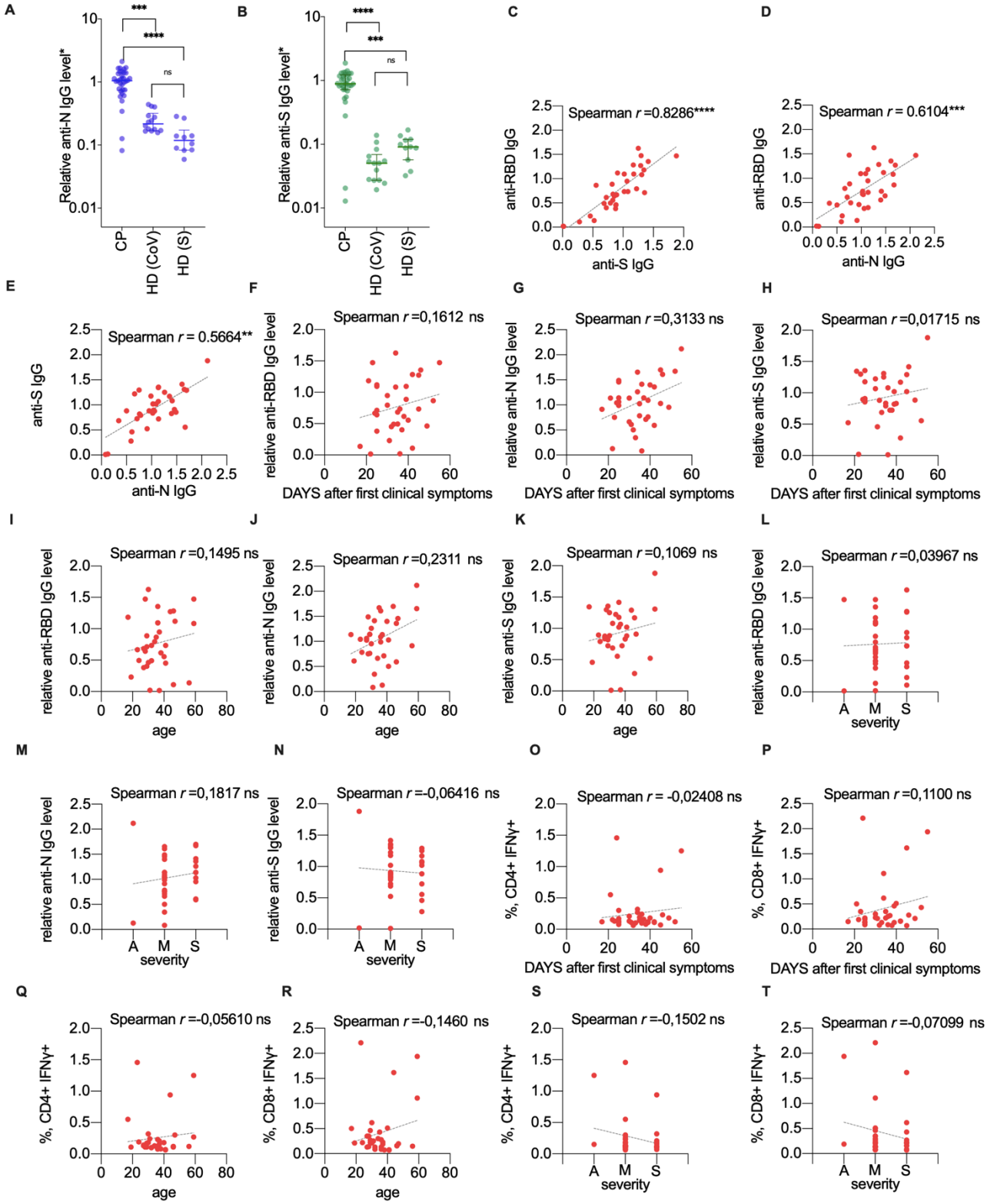

Figure S1. Antibody and T cell response to the different SARS-CoV-2 antigens. Related to Figure 1.
(A and B) Measurement of detection antibodies to (A) N protein and (B) full-length S protein with an in-house ELISA assay. OD_{650} was subtracted from OD_{450} for each well. Mean OD for each serum sample was divided to determine the normalizing coefficient (EC_{50} of the calibration curve) in order to compare the samples across different plates.
(C-E) The Spearman correlation and linear regression between (C) anti-RBD and anti-S IgG, (D) anti-RBD and anti-N IgG, (E) and anti-S and anti-N IgG are shown (CP cohort). For group comparison, Kruskal–Wallis test and Dunn's multiple comparison test were used. RBD = receptor binding domain; CP = convalescent patients; HD(CoV) - healthy donors sampled during COVID-19 pandemic; and HD(S) = biobanked healthy donor serum. (F-H) Correlation between antibody response and time after the onset of disease or positive PCR test. Spearman's coefficient of correlation between time and relative levels of (F) anti-RBD, (G) anti-N, (H) anti-S IgGs and linear regression is plotted (n = 34). (I–K) Correlation between antibody response and CP age. Spearman's coefficient of correlation between age and relative levels of (I) anti-RBD, (J) anti-N, (K) anti-S IgGs and linear regression is plotted (n = 34).
(L–N) Correlation between antibody response and severity of disease in CPs. Spearman's coefficient of correlation between asymptomatic (A), mild (M) and moderate/severe (S) groups and relative levels of (L) anti-RBD, (M) anti-N, and (N) anti-S IgGs and linear regression is plotted (n = 34). (O–P) Correlation between T cell response and time after onset of the disease or positive PCR test. Spearman's coefficient of correlation between time and frequencies of IFNγ-producing (O) $CD4^+$ or (P) $CD8^+$ T cells and time, with linear regression plotted (n = 34). (Q–R) Correlation between T cell response and age. Spearman's coefficient of correlation between age and frequencies of IFNγ-producing (Q) $CD4^+$ or (R) $CD8^+$ T cells and time, with linear regression plotted (n = 34).
(S–T) Correlation between antibody response and severity of disease in CPs. Spearman's coefficient of correlation between A, M and S groups and frequencies of IFNγ-producing (S) $CD4^+$ or (T) $CD8^+$ T cells and time, with linear regression plotted (n = 34). p-values ***$p < 0.001$, ****$p < 0.0001$.

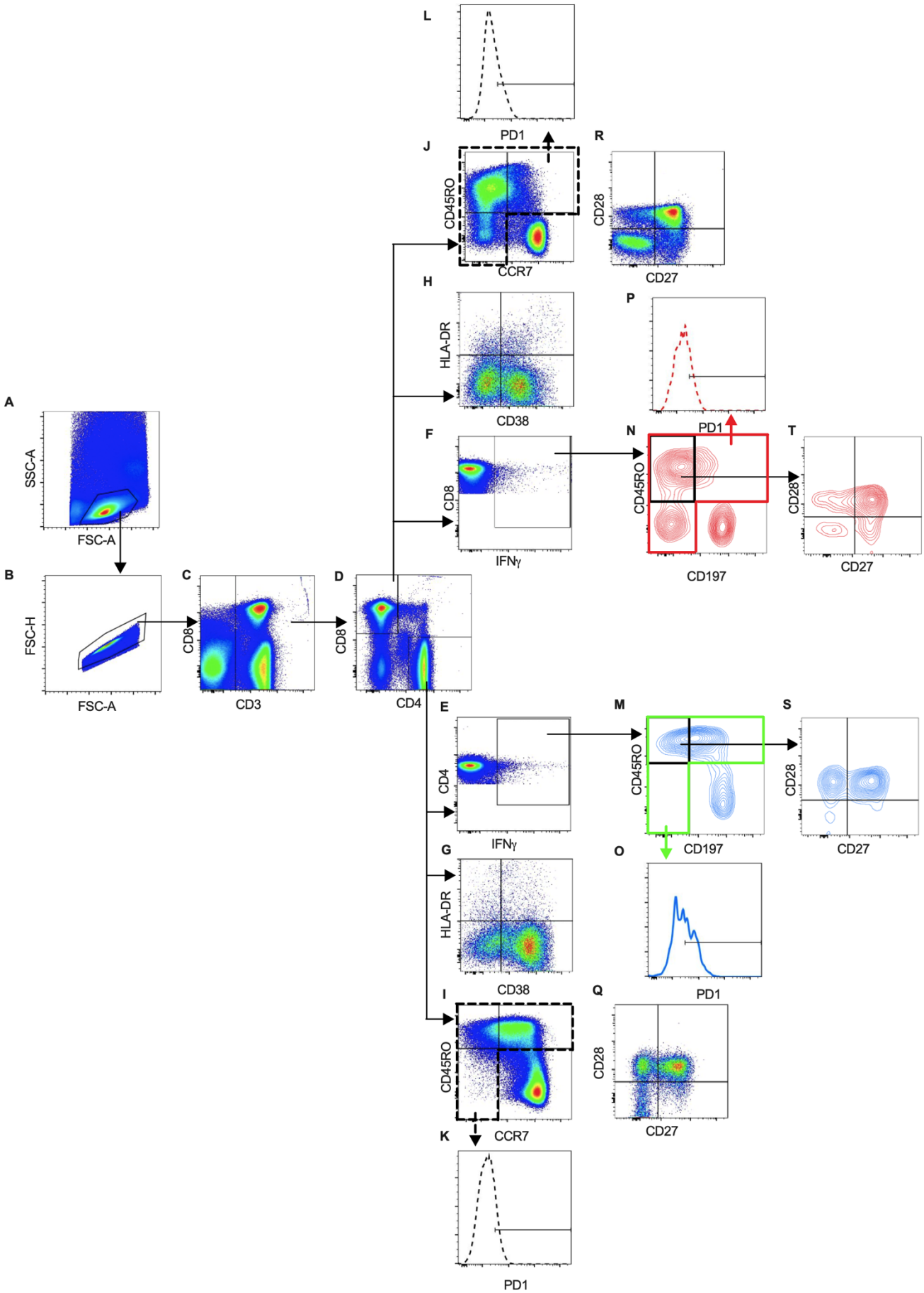
A
SSC-A
FSC-A
B
FSC-H
FSC-A
C
CD8
CD3
D
CD8
CD4
E
CD4
IFNγ
F
CD8
IFNγ
G
HLA-DR
CD38
H
HLA-DR
CD38
I
CD45RO
CCR7
J
CD45RO
CCR7
K
PD1
L
PD1
M
CD45RO
CD197
N
CD45RO
CD197
O
PD1
P
PD1
Q
CD28
CD27
R
CD28
CD27
S
CD28
CD27
T
CD28
CD27

Figure S2. Flow cytometry gating strategy. Related to Figure 1.
(A)Total lymphocytes were gated based on forward scatter (FSC-A)/side scatter (SSC-A).
(B) Singlets were gated based on area and high FSC signal.
(C and D) Major T cell subtypes were gated based on CD3 (C) and CD4/CD8 (D) positivity.
(E-J) CD4+ (E, G and I) and CD8+ (F, H and J) cells were further gated as: total IFNγ-producing cells (E and F); activated cells based on CD38 and HLA-DR expression (G and H); and differentiation subpopulations based on CD45RO and CD197 expression (I and J).
(I-P) PD1 histogram for non-naive CD4+ (I and K) and CD8+ (J and I) cells, and for non-naive IFNγ-producing CD4+ (M and O) and CD8+ (N and P) cells. Gating is also shown for TEM subsets among CD4+ (L and Q), CD8+ (J and R), IFNγ-producing CD4+ (M and S), and IFNγ-producing CD8+ (N and) cells.

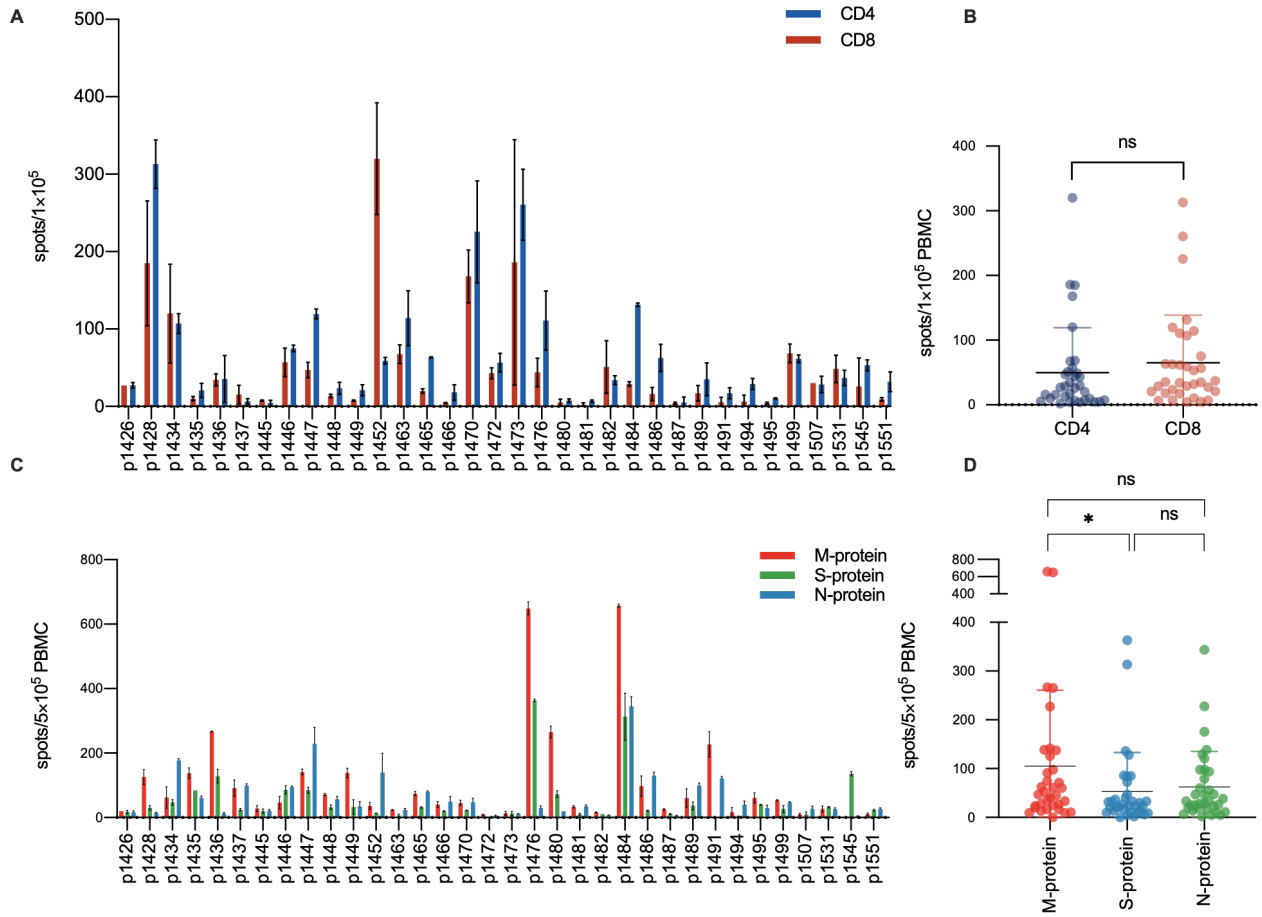

Figure S3. Variability of T cell response to SARS-CoV-2 antigens. Related to Figure 1.
Magnetically separated CD8+ and CD4+ cells and total PBMCs from CPs (n=34) were stimulated with recombinant S protein or with pools of peptides (M, N and S protein) for 18 hours. IFNγ response was assessed by ELISPOT.
(A and B) Number of recombinant S protein-specific CD8+ and CD4+ T cells.
(C and D) Number of M, S or N peptide-specific T cells. Spots were quantified by automated digital image analysis in duplicate wells. Plotted data are means of two independent measurements ± SD. For group comparisons, the data were log(2)-transformed, normality was assessed by Shapiro-Wilk test, and two-way ANOVA with Tukey's multiple comparisons test was performed. *p < 0.05. Negative control is deduced from each value.

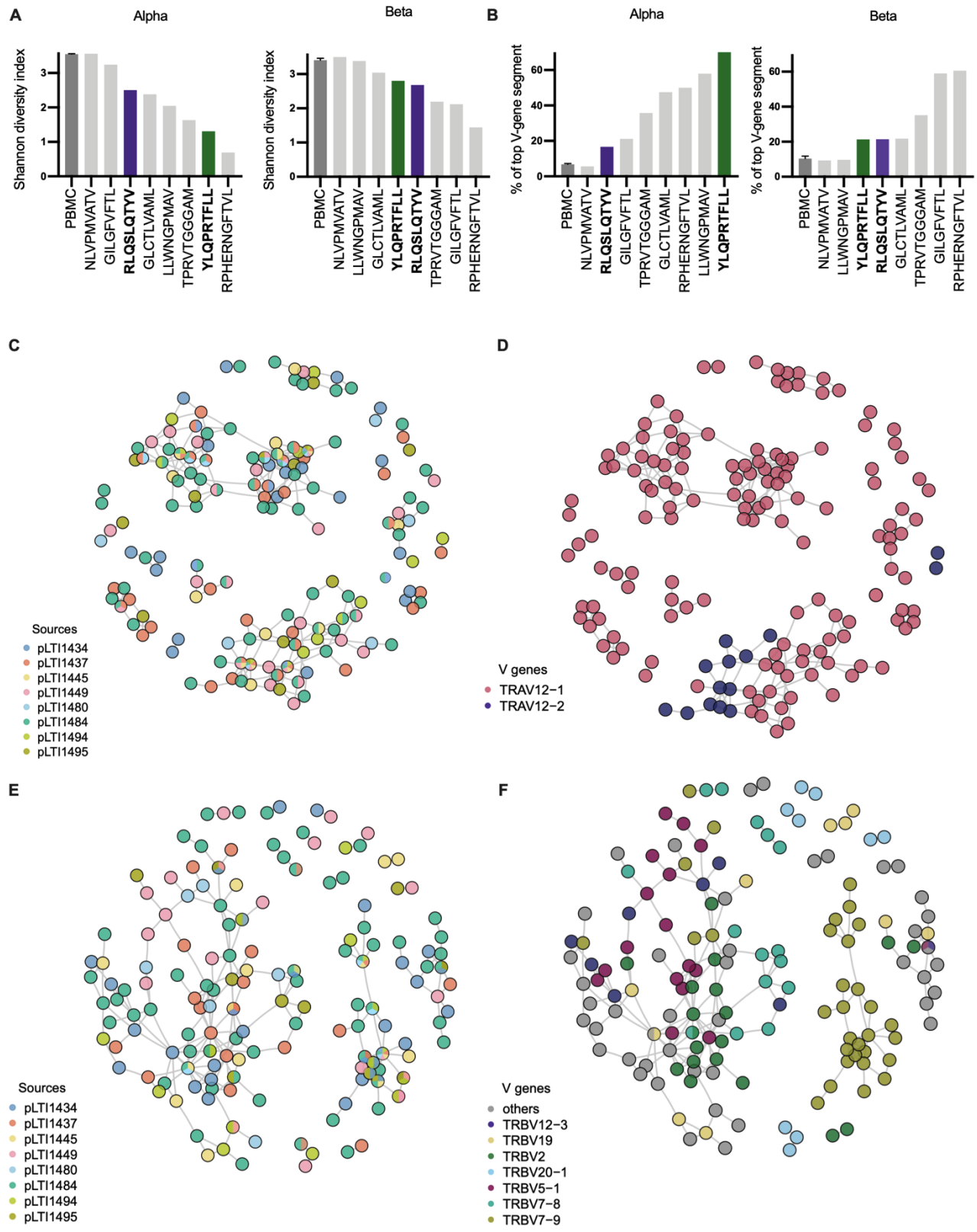

Figure S4 V-gene usage of YLQ and RLQ-specific TCRs and global similarity of YLQ-specific CDR3 amino acid sequences. Related to Figure 3.

(A) Shannon diversity of V-gene usage by α and β chains of TCRs specific to well characterized viral epitopes and to the SARS-CoV-2 S protein epitopes described in this study, RLQ (purple) and YLQ (green).

(B) Fraction of epitope-specific TCRs using the most frequent V-gene segment. Mean of all PBMCs from this study were used as controls ± SD.

(C–F) Global similarity of YLQ-specific CDR3 amino acid sequences. Graph shows CDR3 amino acid sequences of MHC-tetramer-positive clones with Hamming distance of 1 or 0. (C and D) TCRα CDR3 amino acid sequences. (E and F) TCRβ CDR3 amino acid sequences. For C and E, colors correspond to different CPs; for D and F, color corresponds to different V genes. Each dot represents one CDR3 amino acid sequence.

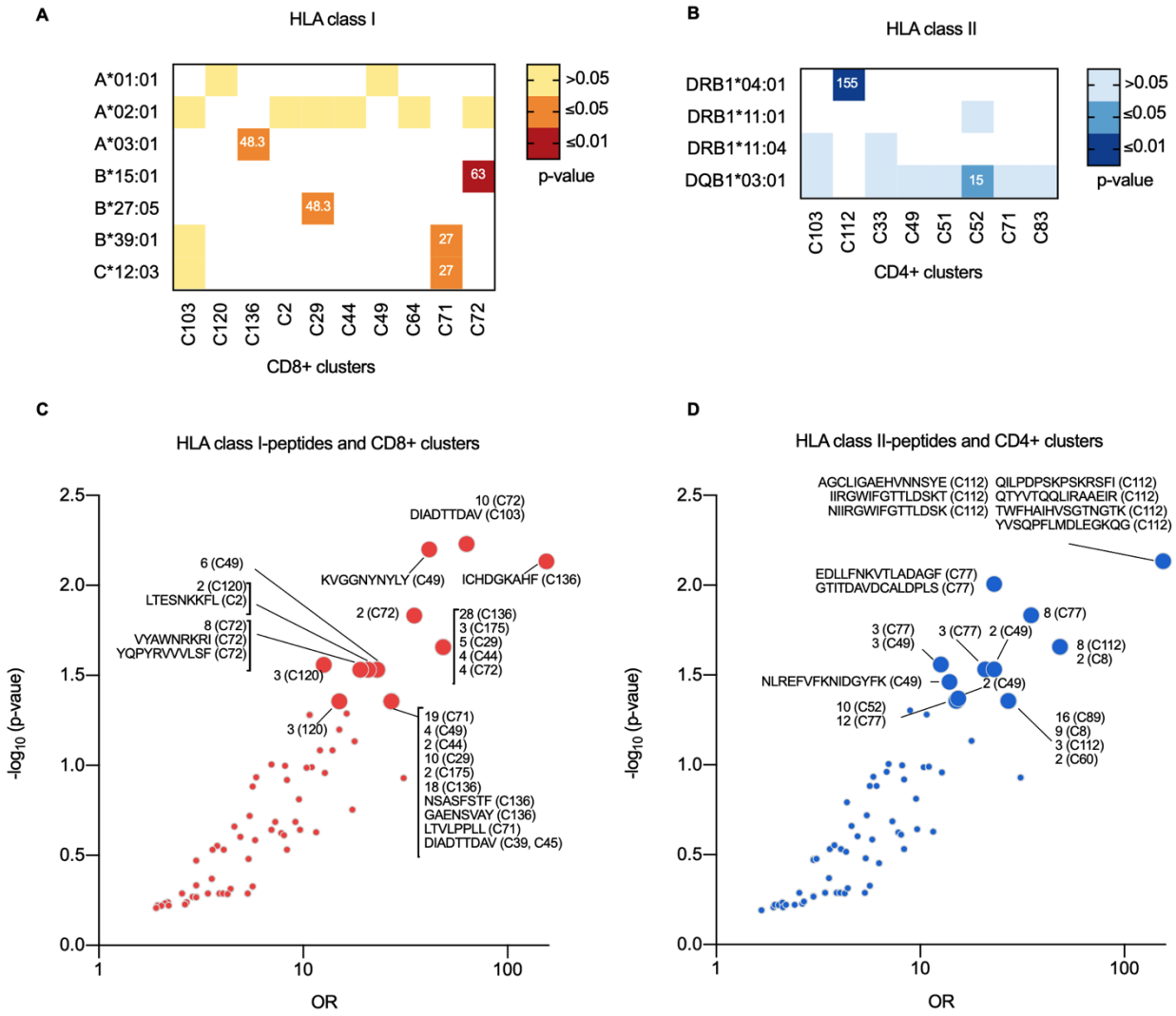

Figure S5. Co-occurrence of HLA alleles and HLA-presented peptides with TCR clusters in convalescent patients. Related to Figure 4.

(A and B) Heatmaps show the association of class I and II HLA alleles and particular CD8++ and CD4++ TCR clusters, respectively. Only positively associated (odds ratio (OR) > 1) cluster-HLA combinations are shown. Color indicates p-value as determined by the exact Fisher test. OR values are indicated for significant associations.

(C and D) Volcano plots depicting the association of a particular peptide potentially presented by patient HLA class I alleles and CD8+ TCR clusters (C) or HLA class II alleles and CD4+ TCR clusters (D). Only positive association (OR>1, -log10 (p-value)>0 by the exact Fisher test) is shown. Datapoints with p-value < 0.05 are shown as large circles. Selected peptide sequences are shown; for other datapoints, the number of peptides is provided. Association with a particular cluster is indicated in parentheses.

Table S1. HLA genotyping. Related to Figure 1.

Table S2. Enriched IFNγ^{+} clones. Related to Figure 2.

Table S3. Homologous TCR clusters. Related to Figure 4.

Table S4. Allele-cluster and allele-peptide co-occurrence. Related to Figure 4